Nuclear Engineering and Technology 54 (2022) 732–740

Contents lists available at ScienceDirect

Nuclear Engineering and Technology

journal homepage: www.elsevier.com/locate/net

Original article

Efficient elastic stress analysis method for piping system with wall-thinning and reinforcement

Ji-Su Kim, Je-Hoon Jang, Yun-Jae Kim*

Mechanical Engineering, Korea University, Seoul, 02841, South Korea

ARTICLE INFO

Article history:
Received 18 May 2021
Received in revised form
3 August 2021
Accepted 21 August 2021
Available online 24 August 2021

Keywords:
Elastic stiffness
Efficient piping system stress analysis
Wall-thinned pipe with reinforcement

ABSTRACT

A piping system stress analysis need to be re-performed for structural integrity assessment after reinforcement of a pipe with significant wall thinning. For efficient stress analysis, a one-dimensional beam element for the wall-thinned pipe with reinforcement needs to be developed. To develop the beam element, this work presents analytical equations for elastic stiffness of the wall-thinned pipe with reinforcement are analytically derived for axial tension, bending and torsion. Comparison with finite element (FE) analysis results using detailed three-dimensional solid models for wall-thinned pipe with reinforcement shows good agreement. Implementation of the proposed solutions into commercial FE programs is explained.

1. Introduction

Thermal and nuclear plants typically have complex piping system and thus design of a piping system is an important issue. Due to complex piping geometries and loading conditions, piping design is typically performed based on the elastic finite element (FE) analysis using one-dimensional beam element. From elastic FE analysis results for all transient loadings, internal forces and moments at a target point in a piping system are obtained, using which fatigue life analysis can be performed using construction codes such as ASME Boiler and Pressure Vessel Code [1]. Note that internal forces and moments in a piping system are affected by the stiffness of a piping system.

During operation, piping components are subject to various degradation mechanisms such as wall thinning or cracking [2–4]. For instance, wall thinning due to erosion and corrosion is a quite popular degradation mechanism. When it is found during service, the continued operation can be checked using some certified codes and standards, for instance, using ASME Code Case N-597-2 [5] for nuclear piping, or using more advanced analysis results. Various works have been done to develop acceptance criteria for wall-thinned pipes; for instance, the effect of wall-thinning on pipe failure pressures [6–10] and bending strength [11–13]. In case when acceptance criteria cannot be met, the defective pipe should be either replaced or repaired. As repair can generally offer cost-effective and time saving, it is more preferred than complete replacement. In several standards such as Code cases N-786 and 789 [14,15], repair methods based on reinforcement using sleeves and pads are provided; the repair using sleeves reinforces the entire perimeter of the pipe, whereas the pad covers the entire shape of the thinning but only a part of the perimeter is reinforced. It has been also shown that reinforcement can increase the strength and load carrying capacity. For instance, it was demonstrated that, by adhesively reinforcing CFRP, the maximum gain of strength in the combined flexural and bearing strength of the pipe was 434% and the load carrying capacity increased by average 97% and 169% [16]. Reinforcing the cracked region of the pressure vessels with a material having higher elastic modulus was shown to be more practical to strengthen the defective structure [17]. In an investigation of the behaviour of composite repaired systems and pipes [18,19], the burst pressure also increased by ~23%.

After repair, however, local stiffness of the piping system should be changed due to the reinforcement and severe wall-thinning on the pipe, which in turn can change overall internal force and moment distributions in a piping system. Thus, these changes in pipe strength resulting from reinforcing defects may require re-analysis of the entire pipe system. It should be noted that, due to its large scale and complexity, piping system stress analysis is typically performed using one-dimensional (1-D) beam elements using piping design exclusive programs [20–23]. Even when full three-dimensional (3-D) FE analysis is needed, it is performed for efficiency using a sub-modelling technique where load or

* Corresponding author.
E-mail address: kimy0308@korea.ac.kr (Y.-J. Kim).

https://doi.org/10.1016/j.net.2021.08.026

Nomenclature

a	depth of wall thinning
A	cross-sectional area
K^P, K_i^B, K^T	elastic stiffness of the wall-thinned pipe with reinforcement for tension, bending ($i = x, y$) and torsion
E^P, E_i^B, E^T	equivalent Young's modulus of pipe for 1D beam element for tension, bending ($i = x, y$) and torsion
E, E^r	Young's modulus of original pipe and reinforcement
G, G^r	shear modulus of original pipe and reinforcement
h^P, h_i^B, h^T	final correction factor for tension, bending ($i = x, y$) and torsion
I	moment of inertia
J	polar moment of inertia
L, l_r, l	length of original pipe, reinforcement and wall-thinning
m^P, m_i^B, m^T	dimensionless variable for tension, bending and torsion
M_i	bending moment for $i = x, y$ and torsion for $i = z$
P	tension
R_i, R_o	inner and outer radius of original pipe
T, t_r	thickness of original pipe and reinforcement
δ	elongation
ϕ_i	bending angle for $i = x, y$ and torsion angle for $i = z$
θ	angle of wall-thinning

Abbreviations

ASME	American Society of Mechanical Engineers
N. A.	neutral axis
FE	finite element

displacement boundary conditions to the model are obtained from the 1-D piping system analysis. Using 3-D FE analysis, Skarakis et al. [24] investigated mechanical performance of a carbon fiber reinforced pipe under severe cyclic loading conditions and showed that the pipe could sustain almost 3.5 times more load cycles with the carbon fiber reinforcement. Chatzopoulou et al. [25] also investigated the effect of carbon fiber reinforcement on mechanical responses of the pipe using 3-D modeling with the solid elements and found that the fatigue life was improved by significantly reducing the hoop strain. Mazurkiewicz et al. [26] evaluated burst pressure of a wall-thinned pipe with fiber glass reinforcement using 3-D FE analysis and showed that local wall-thinned pipe could reduce high pressure resistance. However, analysis should be often performed not for a piping element but for whole piping system. In such cases, the use of 3-D FE analysis is not practical. To perform efficiently a whole piping system (elastic) stress analysis with a region with severe wall-thinning and reinforcement, it is necessary to develop a 1-D beam element equivalent to a wall-thinned pipe with reinforcement, which is the objective of this paper. The equivalency should be based on the concept to match elastic stiffness for forces and moments, so that elastic responses of the one-dimensional beam element to forces and moments are the same as those of a wall-thinned pipe with reinforcement. With such 1-D beam element, a piping system stress analysis can be efficiently performed to find elastic stress redistribution due to wall thinning and reinforcement.

This work presents a method to develop a 1-D beam element equivalent to a wall-thinned pipe with reinforcement for efficient piping system elastic stress analysis after reinforcement. The method is based on analytically determining the stiffness of a wall-thinned pipe with reinforcement. In Section 2, explicit equations for the elastic stiffness of a wall-thinned pipe with reinforcement are analytically derived for axial force and for moments. In Section 3, the validity of the derived solution is checked by comparing with the three-dimensional FE analysis results. Implementation of the present result into computer programs is explained in Section 4. Section 5 concludes the present work.

2. Analytical elastic stiffness solutions of wall-thinned pipe with reinforcement

2.1. Definition of analysis model

An analysis model for a wall-thinned pipe with reinforcement is shown in Fig. 1. The coordinate (x, y, z) is shown in Fig. 1. Relevant dimensions of the pipe are the thickness T; the length L; and inner and outer radius, R_i and R_o. The dimensions of the reinforcement are the reinforcement thickness t_r; and the reinforcement length l_r. The wall-thinning is characterized by its length l, depth a, and half circumferential angle, θ. The distance between the x-axis and the neutral axis is d. For loading, global bending, M_x and M_y, torsion, M_z, and axial tension, P, are considered. The problem is to analytically find expressions of the stiffness for the model shown in Fig. 1.

As the present analysis is to develop elastic stiffness of a wall-thinned pipe with reinforcement, the basic assumption is that pipe and reinforcement materials behave elastically under the small strain (deformation) assumption. In addition, the following assumptions are further made for the present analysis:

(1) Materials of the pipe and reinforcement are assumed to be isotropic.
(2) The reinforcement covers the entire perimeter of the pipe.
(3) The wall-thinning is assumed to have a rectangular shape rather than a circular one.
(4) Welding in the end of the reinforcement is not considered and is modelled a sharp end.

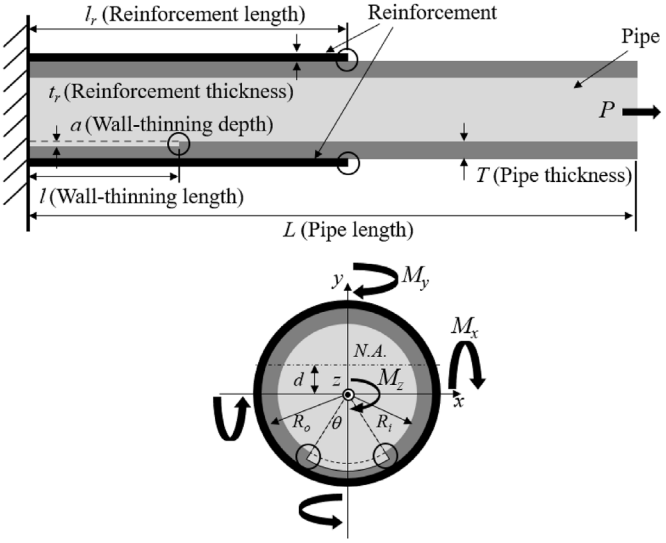

Fig. 1. Schematic illustrations of a wall-thinned pipe with reinforcement.

(5) The wall-thinning is located in the bottom the pipe.

These assumptions are not essential and the results to be presented in this paper can be easily generalized to more general conditions, as will be discussed in Section 2.6.

2.2. Analysis

At the end of the pipe with the total length L, an axial elongation δ under axial tension, P, a rotation angle ϕ for bending, M_x and M_y, and a twisting angle ϕ under torsion M_z is given by

$$\begin{aligned} P &= \frac{E\cdot A}{L}\delta = K^P\cdot\delta \\ M_i &= \frac{E\cdot I_i}{L}\phi_i = K_i^B\cdot\phi_i\,, \quad i=x,\,y \\ M_z &= \frac{G\cdot J}{L}\phi_z = K^T\cdot\phi_z \end{aligned} \tag{1}$$

The tensile stiffness, K^P, is given by the cross-sectional area, A, the Young's modulus, E and the length of the pipe, L. The bending stiffness, K_i^B, is given by the moment of inertia, I_i, instead of the area. The torsional stiffness, K^T, is related with the polar moment of inertia, J, and the shear modulus, G. The key point to calculate the elastic stiffness of a wall-thinned pipe with reinforcement is to calculate an equivalent moment of inertia for bending or torsion and an equivalent area for tension.

Note that the stiffness change due to transverse forces is not considered in this study due to the following reason. Transverse forces typically act as a boundary condition to a piping system, which can produce internal forces and moments. However, it is well known that stresses and strains produced by shear forces are much smaller than those from other types of internal force and moment components and thus that the stiffness change due to internal shear forces can be neglected.

With the assumptions (1) to (4) given in Section 2.1, the wall-thinned pipe with reinforcement can be divided by three sections; the original pipe section (section 1 in Fig. 2); the pipe section with reinforcement (section 2 in Fig. 2); and the wall-thinned pipe section with reinforcement (section 3 in Fig. 2). Using the superposition principle, the elongation or angle can be calculated using

$$\begin{aligned} \delta &= (\delta)_1 + (\delta)_2 + (\delta)_3 \\ \phi_i &= (\phi_i)_1 + (\phi_i)_2 + (\phi_i)_3, \quad i=x,\,y,\,z \end{aligned} \tag{2}$$

or

$$\begin{aligned} \frac{PL}{E(A)_{eq}} &= \frac{P(L-l_r)}{E(A)_1} + \frac{P(l_r-l)}{E(A)_2} + \frac{Pl}{E(A)_3} \\ \frac{M_iL}{E(I_i)_{eq}} &= \frac{M_i(L-l_r)}{E(I)_1} + \frac{M_i(l_r-l)}{E(I)_2} + \frac{M_il}{E(I_i)_3},\ i=x,\,y \\ \frac{M_zL}{G(J)_{eq}} &= \frac{M_z(L-l_r)}{G(J)_1} + \frac{M_z(l_r-l)}{G(J)_2} + \frac{M_zl}{G(J)_3} \end{aligned} \tag{3}$$

where the subscript outside the parentheses denotes the relevant variable for each section in Fig. 2. For example, $(\delta)_1$, $(\delta)_2$ and $(\delta)_3$ in Fig. 2 denote the axial elongation of the pipe with the length of $(L\text{-}l_r)$, $(l_r\text{-}l)$ and l, respectively. Similarly, $(\phi)_1$, $(\phi)_2$, and $(\phi)_3$ in Fig. 2 denote the rotation angle of the pipe with the length of $(L\text{-}l_r)$, $(l_r\text{-}l)$, and l, respectively. In Eq. (3), $(A)_{eq}$, $(I_i)_{eq}$ and $(J)_{eq}$ denotes the equivalent cross-sectional area, bending moment of inertia and torsional moment of inertia for the wall-thinned pipe with reinforcement, respectively. The moment of inertia and cross-sectional area of the pipe in section 1 can be easily calculated. In sections 2 and 3, force equilibrium leads to

$$\begin{aligned} P &= (P)_2^o + (P)_2^r = (P)_3^{wt} + (P)_3^r \\ M_i &= (M_i)_2^o + (M_i)_2^r = (M_i)_3^{wt} + (M_i)_3^r,\ i=x,\,y,\,z \end{aligned} \tag{4}$$

where the superscript in the parentheses refers to; o = original pipe; r = reinforcement; wt = wall-thinning. Equation (4) can be rewritten as

$$\begin{aligned} \frac{E(A)_2}{l_r-l}(\delta)_2 &= \frac{E(A)_2^o}{l_r-l}(\delta)_2 + \frac{E^r(A)_2^r}{l_r-l}(\delta)_2 = \frac{\left(m^P\right)_2E(A)_1}{l_r-l}(\delta)_2 \\ \frac{E(I)_2}{l_r-l}(\phi_i)_2 &= \frac{E(I)_2^o}{l_r-l}(\phi_i)_2 + \frac{E^r(I)_2^r}{l_r-l}(\phi_i)_2 = \frac{\left(m^B\right)_2E(I)_1}{l_r-l}(\phi_i)_2, \text{for } i=x,y \\ \frac{G(J)_2}{l_r-l}(\phi_z)_2 &= \frac{G(J)_2^o}{l_r-l}(\phi_z)_2 + \frac{G^r(J)_2^r}{l_r-l}(\phi_z)_2 = \frac{\left(m^T\right)_2G(J)_1}{l_r-l}(\phi_z)_2 \end{aligned} \tag{5}$$

for section 2 and

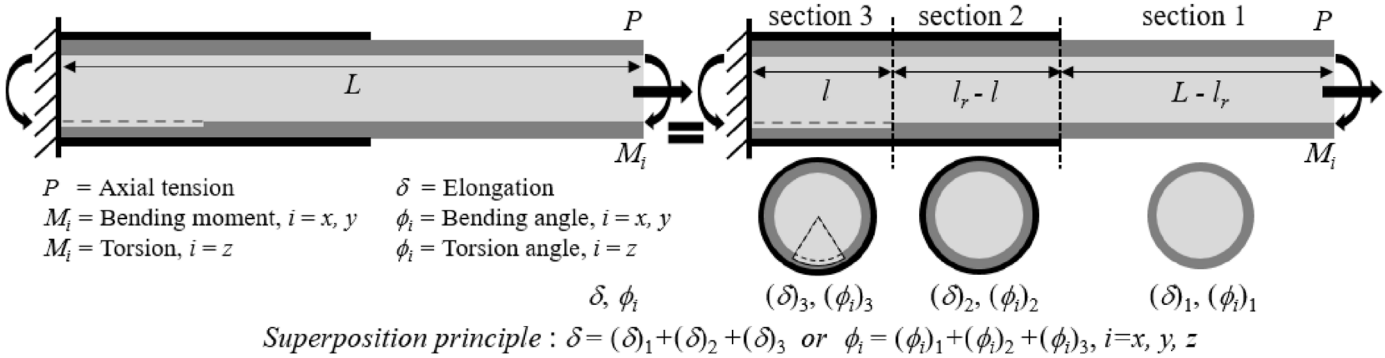

Fig. 2. Schematic illustration of the superposition principle for the wall-thinned pipe with reinforcement.

$$\frac{E(A)_3}{l}(\delta)_3=\frac{E(A)_3^{wt}}{l}(\delta)_3+\frac{E^r(A)_3^r}{l}(\delta)_3=\frac{\left(m^P\right)_3E(A)_1}{l}(\delta)_3$$

$$\frac{E(I_i)_3}{l}(\phi_i)_3=\frac{E(I_i)_3^{wt}}{l}(\phi_i)_3+\frac{E^r(I)_3^r}{l}(\phi_i)_3=\frac{\left(m_i^B\right)_3E(I)_1}{l}(\phi_i)_3, for i=x,y$$

$$\frac{G(J)_3}{l}(\phi_z)_3=\frac{G(J)_3^{wt}}{l}(\phi_z)_3+\frac{G^r(J)_3^r}{l}(\phi_z)_3=\frac{\left(m^T\right)_3G(J)_1}{l}(\phi_z)_3 \tag{6}$$

for section 3, as shown in Fig. 3. Young's modulus and shear modulus for the reinforcement is expressed by E^r and G^r, respectively. Introducing dimensionless variables (m^P, m_i^B and m^T) reflecting the effect of the reinforcement or wall-thinning on the pipe sectional modulus in each section, the equivalent cross-sectional area and moment of inertia for each section of the pipe can be calculated and the results will be given in the subsequent sub-sections.

2.3. Tension stiffness solution

According to Eqs. (5) and (6), the dimensionless variable, m^P, for each pipe section in Fig. 2 is given by

$$\left(m^P\right)_2=1+\frac{E^r(A)_2^r}{E(A)_1},\quad \left(m^P\right)_3=\frac{(A)_3^{wt}}{(A)_1}+\frac{E^r(A)_3^r}{E(A)_1} \tag{7}$$

where the effect of the reinforcement on the sectional modulus in section 2 pipe is corrected by $(m^P)_2$ and that of the wall thinning with the reinforcement in section 3 pipe is corrected by $(m^P)_3$.

Using Eqs. (3) and (7), the equivalent cross-sectional area for the wall-thinned pipe with reinforcement, $(A)_{eq}$, is given by

$$(A)_{eq}=\frac{(m^P)_2\cdot(m^P)_3\cdot L}{(m^P)_2\cdot(m^P)_3(L-l_r)+(m^P)_3(l_r-l)+(m^P)_2(l)}\cdot(A)_1 = h^P\cdot(A)_1 \tag{8}$$

where h^P denotes a final correction factor and $(A)_1$ denotes the cross-sectional area of the original pipe. The tensile stiffness K^P is given by

$$\frac{P}{\delta}=K^P=\frac{E\cdot(A)_{eq}}{L}=\frac{E\cdot h^P\cdot(A)_1}{L} \tag{9}$$

2.4. Bending stiffness solution

For bending moment, the dimensionless variable, m_i^B, for each section of the pipe in Fig. 2 is given by

$$\left(m^B\right)_2=1+\frac{E^r(I)_2^r}{E(I)_1},\quad \left(m_i^B\right)_3=\frac{(I_i)_3^{wt}}{(I)_1}+\frac{E^r(I)_3^r}{E(I)_1},\ i=x,\ y \tag{10}$$

The equivalent moment of inertia under bending is given by

$$(I_i)_{eq}=\frac{(m^B)_2\cdot(m_i^B)_3\cdot L}{(m^B)_2\cdot\left(m_i^B\right)_3(L-l_r)+\left(m_i^B\right)_3(l_r-l)+(m^B)_2(l)}\cdot(I)_1 = h_i^B\cdot(I)_1,\ i=x,\ y \tag{11}$$

where the final correction factor under bending is characterized by h_i^B. The cross-sectional area in Eqs. (7) and (8) is simply replaced with the moment of inertia in Eqs (10) and (11). Thus, the bending stiffness K_i^B is as follows:

$$\frac{M_i}{\phi_i}=K_i^B=\frac{E\cdot(I_i)_{eq}}{L}=\frac{E\cdot h_i^B\cdot(I)_1}{L},\quad i=x,\ y \tag{12}$$

2.5. Torsional stiffness solution

Similar to bending, the dimensionless variable, m^T, for each section of the pipe in Fig. 2 is given by

$$\left(m^T\right)_2=1+\frac{G^r(J)_2^r}{G(J)_1},\quad \left(m^T\right)_3=\frac{(J)_3^{wt}}{(J)_1}+\frac{G^r(J)_3^r}{G(J)_1} \tag{13}$$

where the shear modulus and polar moment of inertia are used, instead of Young's modulus and moment of inertia in Eq. (10). The equivalent polar moment of inertia under torsion is given by

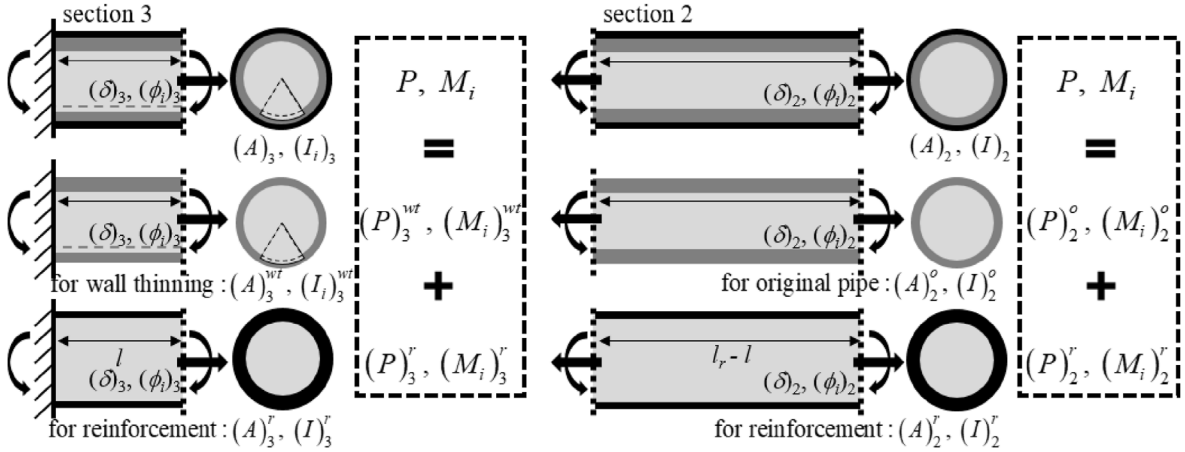

Fig. 3. Application of the superposition principle to the original pipe, reinforcement and wall-thinned pipe in section 2 and 3.

$$(J)_{eq} = \frac{(m^T)_2 \cdot (m^T)_3 \cdot L}{(m^T)_2 \cdot (m^T)_3 (L - l_r) + (m^T)_3 (l_r - l) + (m^T)_2 (l)} \cdot (J)_1 = h^T \cdot (J)_1 \tag{14}$$

The torsional stiffness K^T is given by

$$\frac{M_z}{\phi_z} = K^T = \frac{G \cdot (J)_{eq}}{L} = \frac{G \cdot h^T \cdot (J)_1}{L} \tag{15}$$

2.6. Discussion on assumptions

In the previous sub-sections, the effect of the wall-thinning geometry and reinforcement on elastic stiffness has been theoretically derived. Several assumptions have been made in derivation, as listed in Section 2.1.

(1) Materials of the pipe and reinforcement are assumed to be isotropic.
(2) The reinforcement covers the entire perimeter of the pipe.
(3) The wall-thinning is assumed to have a rectangular shape rather than a circular one.
(4) Welding in the end of the reinforcement is not considered and is modelled a sharp end.
(5) The wall-thinning is located in the bottom the pipe.

For the first assumption, the analysis could be generalized to the case when reinforcement material is anisotropic but is expected to be quite complicated. Other than the assumption (1), other assumptions are not crucial and the analysis can be easily extended, as described below.

The assumption (2) can be released simply by calculating an appropriate moment of inertia in section 2 and section 3 in Fig. 2, considering the coverage of reinforcement. For the assumption (3), typical wall-thinning shape is either circular or semi-elliptical rather than rectangular which is assumed in the present work. For an arbitrary wall-thinning shape, a key is again to calculate an appropriate moment of inertia for the pipe with an arbitrary wall-thinned pipe. Rahman [27] has presented a closed-form solution to calculate the moment of inertia for a pipe with an arbitrary-shaped circumferential surface crack (see also Ref. [28]). The same equation can be used to calculate the moment of inertia for the pipe with an arbitrary wall-thinned pipe. For the assumption (4) when welding is considered in the end of reinforcement, the length of reinforcement, l_r (in Fig. 2), can be adjusted accordingly. For instance, for a triangular shape of welding, half of the weld length can be considered as reinforcement based on an equivalent area. The assumption (5) again can be released simply by calculating an appropriate moment of inertia in section 3 in Fig. 2.

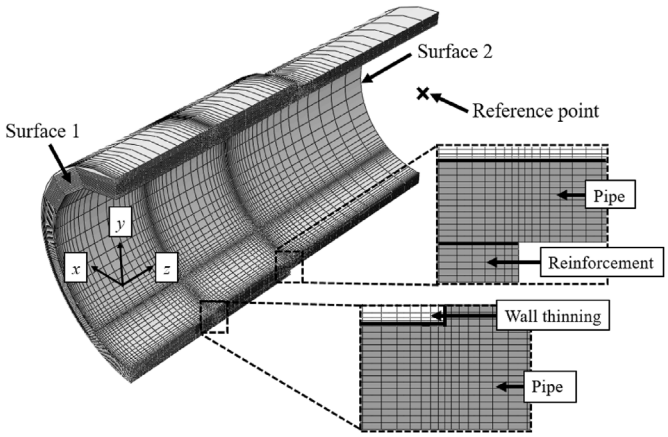

Fig. 4. 3-D FE model of the wall-thinned pipe with reinforcement.

3. Finite element (FE) validation

3.1. Finite element analysis

For validation of the proposed equations, detailed three-dimensional (3-D) elastic FE analysis is performed for the wall-thinned pipe with reinforcement. A typical FE mesh is shown in Fig. 4. A full model was considered with twenty-node solid element with reduced integrations (C3D20R in ABAQUS). For analysis, the length, outer radius and thickness of the pipe was assumed to be $L = 1625.6$ mm, $R_o = 406.4$ mm and $T = 50.8$ mm, respectively. Note that the pipe radius-to-thickness ratio was $R_o/T = 8$ and the length-to-radius ratio was $L/R_o = 4$. Other dimensions for the analysis are summarized in Table 1. A total of 24 cases were considered. In Fig. 4, all degree-of-freedoms of the nodes in the surface 1 were fixed and those of the nodes in the surface 2 were constrained to a reference point located at the center of the pipe using the multi-point constraints (MPC) option in ABAQUS. The concentrated force or moment was applied to the reference point using the CLOAD option in ABAQUS. In the thickness direction, thirteen elements were used in the wall-thinned area and eight elements in the reinforcement. The number of elements and nodes in the mesh ranged from 86,080 elements/364,505 nodes to 112,700 elements/471,501 nodes. The elastic modulus of the original pipe and the reinforcement was set to be 200 GPa. The Poisson's ratio was assumed to be 0.3 for both materials.

3.2. Results

For the wall-thinned pipe with reinforcement under tension, the calculated stiffness using the proposed equations for the cases given in Table 1 are compared with FE results in Fig. 5. The stiffness of the wall-thinned pipe with reinforcement, K^P, is normalized with

Table 1
FE analysis cases.

Dimensions					
R_o/L	Thickness ratio (reinforcement/pipe) t_r/T	Relative thinning angle θ/π	Relative thinning depth a/T	Relative thinning length (thinning/pipe) l/L	Relative reinforcement length (reinforcement/thinning) l_r/l
0.25	0.5	1/6	0.25, 0.75	0.125	1.5
				0.25	1
					1.5
				0.5	1
					1.5
				0.75	1

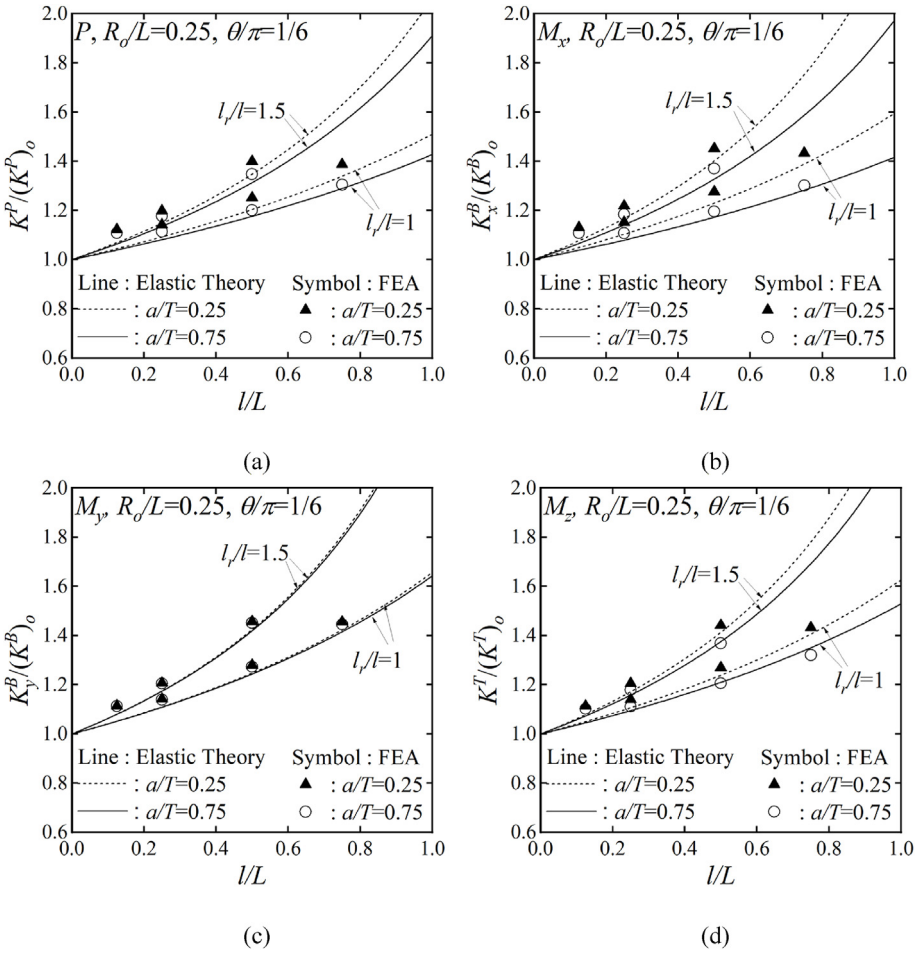

Fig. 5. Comparison of the theoretical stiffness and FE analysis results using 3D elements under (a) tension, P (b) moment, M_x, (c) moment, M_y and (d) torsion, T for $a/T = 0.25$ and $a/T = 0.75$.

respect to that of the original pipe with the same length, radius and thickness, $(K^P)_o$. According to Eqs. (8) and (9), the normalized stiffness under tension can be express by the final correction factor, h^P, as follows:

$$\frac{K^P}{\left(K^P\right)_o}=\frac{\frac{E\cdot h^P\cdot(A)_1}{L}}{\frac{E\cdot(A)_1}{L}}=h^P=\frac{1}{1-\left\{\left[1-\frac{1}{(m^P)_2}\right]\frac{l_r}{l}+\left[\frac{1}{(m^P)_2}-\frac{1}{(m^P)_3}\right]\right\}\frac{l}{L}} \tag{16}$$

It shows that the normalized stiffness, $K^P/(K^P)_o$, depends on the dimensions and properties of the wall-thinned pipe and reinforcement. The normalized stiffness increases with increasing l_r/l, as can be seen in Fig. 5(a). This is obvious because the longer reinforcement length gives the stiffness. On the other hand, the deeper thinning depth means lower pipe stiffness, and thus the normalized stiffness for $a/t = 0.75$ is smaller than that for $a/t = 0.25$, although the effect of a/t on the normalized stiffness is not so large. The longer thinning length gives the lower stiffness. However, as the wall-thinned region is always covered with reinforcement, the stiffness increases even with increasing thinning length, simply due to the reinforcement effect. Comparing the results from the proposed equation with FE results using 3-D solid elements, the maximum error is found to be ~4%, validating the proposed equations.

Corresponding results are shown in Fig. 5(b)–(c) for bending moments and in Fig. 5(d) for torsion. According to Eqs. (12) and (15), the stiffness of the wall-thinned pipe with reinforcement, K_i^B and K^T, normalized with respect to that of the original pipe, $(K_i^B)_o$ and $(K^T)_o$, is given by

$$\frac{K_i^B}{\left(K^B\right)_o}=\frac{\frac{E\cdot h_i^B\cdot(I)_1}{L}}{\frac{E\cdot(I)_1}{L}}=h_i^B=\frac{1}{1-\left\{\left[1-\frac{1}{(m^B)_2}\right]\frac{l_r}{l}+\left[\frac{1}{(m^B)_2}-\frac{1}{(m_i^B)_3}\right]\right\}\frac{l}{L}},\ i=x,y \tag{17}$$

$$\frac{K^T}{\left(K^T\right)_o}=\frac{\frac{G\cdot h^T\cdot(J)_1}{L}}{\frac{G\cdot(J)_1}{L}}=h^T=\frac{1}{1-\left\{\left[1-\frac{1}{(m^T)_2}\right]\frac{l_r}{l}+\left[\frac{1}{(m^T)_2}-\frac{1}{(m^T)_3}\right]\right\}\frac{l}{L}} \tag{18}$$

The form of Eqs. (17) and (18) is quite similar to that of Eq. (16), and thus the same dependence on the variables can be found as in tension. Comparing the results from the proposed equation with FE results using 3-D solid elements, the maximum error is found to be ~4%, which is similar to tension.

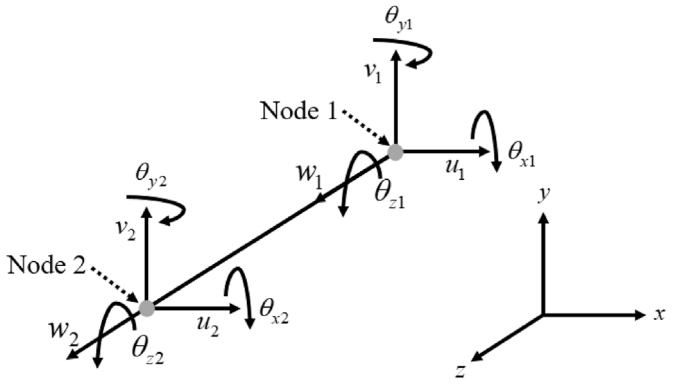

Fig. 6. Degrees of freedom for beam element.

4. Implementation to commercial FE programs

4.1Piping system stress analysis programs

In piping design exclusive programs [20–23], one dimensional beam element is typically used for piping system stress analysis. As shown in Fig. 6, the beam element with six degrees of freedom for each node can be subjected to axial tension, bending moment and torsion. The relationship between the applied load and corresponding deformation can be expressed using the stiffness matrix as follows:

$$\mathbf{F}=\mathbf{K}\cdot\mathbf{U},\quad \begin{Bmatrix}\mathbf{F_1}\\ \mathbf{F_2}\end{Bmatrix}=\begin{bmatrix}\mathbf{K_{aa}} & \mathbf{K_{ab}}\\ \mathbf{K_{ba}} & \mathbf{K_{bb}}\end{bmatrix}\begin{Bmatrix}\mathbf{u_1}\\ \mathbf{u_2}\end{Bmatrix} \tag{19}$$

Assuming that all degrees of freedom for node 2 are constrained for simplicity, the above equation can be written as

$$\mathbf{F_1}=\mathbf{K_{aa}}\cdot\mathbf{u_1},\quad \begin{Bmatrix}F_{z1}\\ F_{x1}\\ F_{y1}\\ M_{z1}\\ M_{x1}\\ M_{y1}\end{Bmatrix}=\begin{bmatrix}\frac{EA}{L} & 0 & 0 & 0 & 0 & 0\\ & \frac{12EI_y}{L^3} & 0 & 0 & 0 & \frac{6EI_y}{L^2}\\ & & \frac{12EI_x}{L^3} & 0 & -\frac{6EI_x}{L^2} & 0\\ & & & \frac{GJ}{L} & 0 & 0\\ & Sym. & & & \frac{4EI_x}{L} & 0\\ & & & & & \frac{4EI_y}{L}\end{bmatrix}\begin{Bmatrix}w_1\\ u_1\\ v_1\\ \theta_{z1}\\ \theta_{x1}\\ \theta_{y1}\end{Bmatrix} \tag{20}$$

where the moment of inertia should be defined according to the load direction. In commercial finite element programs for piping system analysis, the above stiffness matrix can be directly modified. To reflect the effect of wall-thinning and reinforcement on the stiffness matrix, the equivalent stiffness presented in Eqs. (9), (12) and (15) can be used as follows:

$$\begin{Bmatrix}F_{z1}\\ F_{x1}\\ F_{y1}\\ M_{z1}\\ M_{x1}\\ M_{y1}\end{Bmatrix}=\begin{bmatrix}\frac{EAh^P}{L} & 0 & 0 & 0 & 0 & 0\\ & \frac{12EIh_y^B}{L^3} & 0 & 0 & 0 & \frac{6EIh_y^B}{L^2}\\ & & \frac{12EIh_x^B}{L^3} & 0 & -\frac{6EIh_x^B}{L^2} & 0\\ & & & \frac{GJh^T}{L} & 0 & 0\\ & Sym. & & & \frac{4EIh_x^B}{L} & 0\\ & & & & & \frac{4EIh_y^B}{L}\end{bmatrix}\begin{Bmatrix}w_1\\ u_1\\ v_1\\ \theta_{z1}\\ \theta_{x1}\\ \theta_{y1}\end{Bmatrix} \tag{21}$$

where the sectional area and the moment of inertia is revised by the final correction factors given in Eqs. (8), (11) and (14). The modified stiffness matrix of the node includes the effect of wall-thinning and reinforcement and piping system stress analysis can be performed using one-dimensional beam element.

4.2. Application example

An application example for the use of the modified stiffness matrix proposed in this paper is briefly described in this subsection. For the example, a piping system analyzed in Ref. [29] is considered, as shown in Fig. 7. Depending on the purpose of the analysis, the piping system may require detailed 3-D modelling, but in this study, the system is assumed to be modelled using 1-D beam elements. Furthermore, wall thinning with reinforcement is assumed in a straight pipe, as shown in Fig. 7. The straight pipe can consist of several beam elements. Also, the wall-thinning and the reinforcement may exist anywhere in a straight pipe.

For the analysis, the node should be located in the center of the wall thinning region (node 2) and other two nodes (node 1 and node 3) with the distance of L to the left and right side, as shown in Fig. 7. For the analysis, the stiffness matrix [K] and length should be given for each element. For the two elements (element 1 and element 2) including the wall thinning and reinforcement, the modified stiffness matrix developed in this paper (see Eq. (21)) should be used together with the length *L*. For the other elements, on the other hand, the normal stiffness (see Eq. (20) should be used together with the length of each element.

5. Conclusions

After reinforcement of a pipe with significant wall thinning, a piping system stress analysis may need to be re-performed for structural integrity assessment. As detailed three-dimensional modelling of the wall-thinned pipe with reinforcement is difficult and not possible in typical piping design exclusive programs, development of a one-dimensional beam element producing the same elastic responses as a three-dimensional model of the wall-thinned pipe with reinforcement would be desirable.

To develop the beam element, analytical equations for elastic stiffness of the wall-thinned pipe with reinforcement are analytically derived for axial tension, bending and torsion. The developed equations include the effect of the geometry and material properties of wall thinning and reinforcement. To check their validity, the

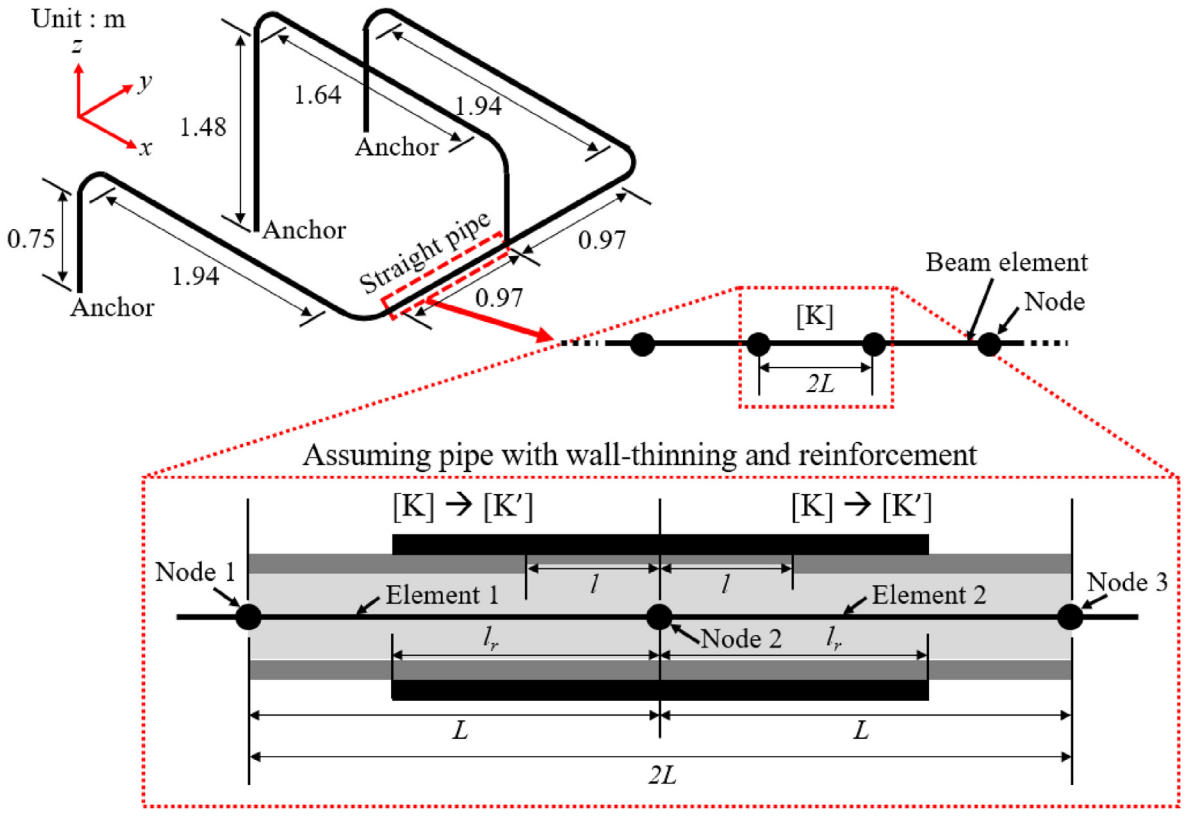

Fig. 7. Schematic illustration of a piping system [29] for an application example of the present approach.

developed solutions are compared with elastic FE analysis results using detailed three-dimensional solid models for wall-thinned pipe with reinforcement, showing good agreement within ~4%.

Finally, implementation of the proposed solutions into commercial FE programs is explained. For piping design exclusive programs, the proposed solutions can be directly used to modify the stiffness matrix of the beam element. For other commercial FE programs, however, incorporation of the present results into the beam element is not possible at present, unless the stiffness matrix is permitted to be modified.

Declaration of competing interest

The authors declare that they have no known competing financial interests or personal relationships that could have appeared to influence the work reported in this paper.

Acknowledgement

This work was supported by Korea Institute of Energy Technology Evaluation and Planning (KETEP) grant funded by the Korea government (MOTIE) (No. 20206510100030, Development of Repair Technology for Class 2, 3 Large Bore Piping in Operating Nuclear Power Plant).

References

[1] ASME Boiler and Pressure Vessel Code, Section III, Rules for Construction of Nuclear Power Plant Components, American Society of Mechanical Engineers, 2015.
[2] J.J. Duffy, M.R. Mahoney, K.M. Steel, Influence of thermoplastic properties on coking pressure generation: Part 1 - a study of single coals of various rank, Fuel 89 (7) (2010) 1590–1599, https://doi.org/10.1016/j.fuel.2009.08.031.
[3] J.W. Kim, C.Y. Park, An experimental study on the evaluation of failure behavior of pipe with local wall thinning, in: Am. Soc. Mech. Eng. Press. Vessel. Pip. Div. PVP, 2002, pp. 9–15, https://doi.org/10.1115/PVP2002-1258, 46512.
[4] J.W. Kim, C.Y. Park, Effect of length of thinning area on the failure behavior of carbon steel pipe containing a defect of wall thinning, Nucl. Eng. Des. 220 (3) (2003) 274–284, https://doi.org/10.1016/S0029-5493(02)00386-2.
[5] ASME Section XI Code Case N-597-2, Requirement for Analytical Evaluation of Pipe Wall Thinning, Am. Soc. of Mech. Eng., New York, USA, 2003.
[6] J.W. Kim, S.H. Lee, C.Y. Park, Experimental evaluation of the effect of local wall thinning on the failure pressure of elbows, Nucl. Eng. Des. 239 (12) (2009) 2737–2746, https://doi.org/10.1016/j.nucengdes.2009.10.003.
[7] J.W. Kim, Y.S. Na, S.H. Lee, Experimental evaluation of the bending load effect on the failure pressure of wall-thinned elbows, J. Press. Vessel Technol. Trans. ASME. 131 (3) (2009), 031210, https://doi.org/10.1115/1.3122032.
[8] J.W. Kim, M.S. Yoon, C.Y. Park, The effect of load-controlled bending load on the failure pressure of wall-thinned pipe elbows, Nucl. Eng. Des. 265 (2013) 174–183, https://doi.org/10.1016/j.nucengdes.2013.07.027.
[9] M. Kamaya, T. Suzuki, T. Meshii, Normalizing the influence of flaw length on failure pressure of straight pipe with wall-thinning, Nucl. Eng. Des. 238 (1) (2008) 8–15, https://doi.org/10.1016/j.nucengdes.2007.06.006.
[10] M. Kamaya, T. Suzuki, T. Meshii, Failure pressure of straight pipe with wall thinning under internal pressure, Int. J. Pres. Ves. Pip. 85 (9) (2008) 628–634, https://doi.org/10.1016/j.ijpvp.2007.11.005.
[11] D.J. Shim, J.B. Choi, Y.J. Kim, Failure strength assessment of pipes with local wall thinning under combined loading based on finite element analyses, J. Press. Vessel Technol. Trans. ASME. 126 (2) (2004) 179–183, https://doi.org/10.1115/1.1687382.
[12] D.J. Shim, Y.J. Kim, Y.J. Kim, Reference stress based approach to predict failure strength of pipes with local wall thinning under combined loading, J. Press. Vessel Technol. Trans. ASME. 127 (1) (2005) 76–83, https://doi.org/10.1115/1.1849228.
[13] Y.J. Kim, D.J. Shim, H. Lim, Y.J. Kim, Reference stress based approach to predict failure strength of pipes with local wall thinning under single loading, J. Press. Vessel Technol. Trans. ASME. 126 (2) (2004) 194–201, https://doi.org/10.1115/1.1687379.
[14] ASME Section XI Code Case N-786-3, Alternative Requirements for Sleeve Reinforcement of Class 2 and 3 Moderate-Energy Carbon Steel Piping for Raw Water Service, Am. Soc. of Mech. Eng., New York, USA, 2017.
[15] ASME Section XI Code Case N-789-3, Alternative Requirements for Pad Reinforcement of Class 2 and 3 Moderate-Energy Carbon Steel Piping, Am. Soc. of Mech. Eng., New York, USA, 2017.

[16] M. Elchalakani, A. Karrech, H. Basarir, M.F. Hassanein, S. Fawzia, CFRP strengthening and rehabilitation of corroded steel pipelines under direct indentation, Thin-Walled Struct. 119 (2017) 510–521, https://doi.org/10.1016/j.tws.2017.06.013.

[17] E. Alizadeh, M. Dehestani, Analytical and numerical fracture analysis of pressure vessel containing wall crack and reinforcement with CFRP laminates, Thin-Walled Struct. 127 (2018) 210–220, https://doi.org/10.1016/j.tws.2018.02.009.

[18] K.S. Lim, S.N.A. Azraai, N. Yahaya, N. Md Noor, L. Zardasti, J.H.J. Kim, Behaviour of steel pipelines with composite repairs analysed using experimental and numerical approaches, Thin-Walled Struct. 139 (2019) 321–333, https://doi.org/10.1016/j.tws.2019.03.023.

[19] M. Xia, K. Kemmochi, H. Takayanagi, Analysis of filament-wound fiber-reinforced sandwich pipe under combined internal pressure and thermomechanical loading, Compos. Struct. 51 (3) (2001) 273–283, https://doi.org/10.1016/S0263-8223(00)00137-9.

[20] A. Ravikiran, P.N. Dubey, M.K. Agrawal, G.R. Reddy, K.K. Vaze, Evaluation of inelastic seismic response of a piping system using a modified iterative response spectrum method, J. Press. Vessel Technol. Trans. ASME. 135 (4) (2013), 041801, https://doi.org/10.1115/1.4023730.

[21] A. Ravikiran, P.N. Dubey, M.K. Agrawal, G.R. Reddy, R.K. Singh, K.K. Vaze, Experimental and numerical studies of ratcheting in a pressurized piping system under seismic load, J. Press. Vessel Technol. Trans. ASME. 137 (3) (2015), 031011, https://doi.org/10.1115/1.4028619.

[22] A. Ravi Kiran, G.R. Reddy, M.K. Agrawal, Seismic fragility analysis of pressurized piping systems considering ratcheting: a case study, Int. J. Pres. Ves. Pip. 169 (2019) 26–36, https://doi.org/10.1016/j.ijpvp.2018.11.013.

[23] A. Ravi Kiran, G.R. Reddy, M.K. Agrawal, M. Raj, S.D. Sajish, Ratcheting based seismic performance assessment of a pressurized piping system: experiments and analysis, Int. J. Pres. Ves. Pip. 177 (2019), 103995, https://doi.org/10.1016/j.ijpvp.2019.103995.

[24] I. Skarakis, G. Chatzopoulou, S.A. Karamanos, N.G. Tsouvalis, A.E. Pournara, CFRP reinforcement and repair of steel pipe elbows subjected to severe cyclic loading, J. Press. Vessel Technol. Trans. ASME. 139 (5) (2017), 051403, https://doi.org/10.1115/1.4037198.

[25] G. Chatzopoulou, I. Skarakis, S.A. Karamanos, N.G. Tsouvalis, A.E. Pournara, Numerical simulation of CFRP reinforced steel pipe elbows subjected to cyclic loading, in: Am. Soc. Mech. Eng. Press. Vessel. Pip. Div. PVP, 2016, 50398, https://doi.org/10.1115/PVP2016-63853. V003T03A027.

[26] L. Mazurkiewicz, M. Tomaszewski, J. Malachowski, K. Sybilski, M. Chebakov, M. Witek, P. Yukhymets, R. Dmitrienko, Experimental and numerical study of steel pipe with part-wall defect reinforced with fibre glass sleeve, Int. J. Pres. Ves. Pip. 149 (2017) 108–119, https://doi.org/10.1016/j.ijpvp.2016.12.008.

[27] S. Rahman, Net-section-collapse analysis of circumferentially cracked cylinders - Part II: idealized cracks and closed-form solutions, Eng. Fract. Mech. 61 (1998) 213–230, https://doi.org/10.1016/S0013-7944(98)00061-7.

[28] Y.J. Kim, D.J. Shim, K. Nikbin, Y.J. Kim, S.S. Hwang, J.S. Kim, Finite element based plastic limit loads for cylinders with part-through surface cracks under combined loading, Int. J. Pres. Ves. Pip. 80 (7–8) (2003) 527–540, https://doi.org/10.1016/S0308-0161(03)00106-6.

[29] D.J. Chang, J.M. Lee, H.S. Nam, N.S. Huh, Y.J. Kim, H.D. Kweon, J.S. Kim, Effect of damage evaluation method and cyclic hardening models on strain-based fatigue assessment to a piping system under seismic loads, J. Mech. Sci. Technol. 34 (7) (2020) 2833–2844, https://doi.org/10.1007/s12206-020-0616-3.